

# Nucleic acid sensing by an orthogonal reporter system based on homo-DNA

Matthias Stoop, Camille Désiron and Christian J. Leumann\*

University of Bern; Department of Chemistry and Biochemistry; Bern, Switzerland

**Keywords:** homo-DNA, Staudinger reaction, RNA diagnostics, fluorescence sensing, oligonucleotides

We have developed an assay for single strand DNA or RNA detection which is based on the homo-DNA templated Staudinger reduction of the profluorophore rhodamine-azide. The assay is based on a three component system, consisting of a homo-DNA/DNA hybrid probe, a set of homo-DNA reporter strands and the target DNA or RNA. We present two different formats of the assay (Omega probe and linear probe) in which the linear probe was found to perform best with catalytic turnover of the reporter strands (TON: 8) and a match/mismatch discrimination of up to 19. The advantage of this system is that the reporting (homo-DNA) and sensing (DNA) domain are decoupled from each other since the two pairing systems are bioorthogonal. This allows independent optimization of either domain which may lead to higher selectivity in *in vivo* imaging.

## Introduction

Homo-DNA (Fig. 1) is composed of 2',3'-dideoxy- $\beta$ -D-glucopyranosyl nucleosides which are linked in a 4'-6'-fashion via regular phosphodiester units. Its properties have been studied in detail by Eschenmoser et al. in the early nineties during his studies on prebiotic structural alternatives to today's nucleic acids.<sup>1,2</sup> Although homo-DNA differs from natural DNA only by one additional methylene group in the sugar ring, its structural, biophysical and molecular recognition properties were found to deviate substantially from that of the natural nucleic acids. Besides reverse Hoogsteen purine-purine base-pairs, homo-DNA also forms canonical Watson-Crick A-T and G-C base pairs, the thermodynamic stabilities of which were significantly higher than that of natural DNA. An important feature is its inability to cross-pair with natural nucleic acids which is due to intrinsic differences in backbone structure.<sup>3</sup> Thus homo-DNA is a prime example of a bioorthogonal, DNA-like pairing system.

Detection of single stranded DNA and RNA is of great importance not only in clinical diagnostics but also from a fundamental point of view, e.g., for understanding cellular function of RNA by live cell imaging. Specific nucleic acid sequences are most commonly targeted by hybridization probes such as fluorescently labeled linear oligonucleotides or hairpin forming molecular beacons.<sup>4</sup> More recent studies are based on the application of templated chemistry where a reaction is triggered between two oligonucleotide probes hybridizing on adjacent sites on the nucleic acid target.<sup>5</sup> Attractive are templated chemical reactions that de-quench a fluorophore via removal of a covalently attached quencher,<sup>6–9</sup> chemically convert a profluorophore into a fluorophore,<sup>10–22</sup> or de novo generate a fluorescent dye.<sup>23,24</sup> An intriguing

asset of templated reactions is their potential to occur in a catalytic manner, leading to an amplification of the fluorescence signal and, consequently, increased sensitivity.<sup>25</sup> A prerequisite for turnover is dynamic strand exchange which is expected to be optimal at the melting temperature of equally stable substrate/target and product/target complexes. To enable this dynamic equilibrium at reasonable temperatures, decamers or shorter oligonucleotide probes are generally used.<sup>12–14,17,26</sup> The restriction to shorter sequences, however, implies compromised fidelity due to statistical non-uniqueness.

In the context of nucleic acid sensing, we have demonstrated that hybrid molecular beacons consisting of a homo-DNA stem and a natural DNA loop show a reduced level of false positive signals due to in-existent cross-pairing between the homo-DNA stem and the natural nucleic acid matrix.<sup>27</sup> In order to exploit homo-DNA's bioorthogonal pairing properties we have recently used a hybrid molecular beacon that is reporting the presence of a target by inducing a homo-DNA templated reaction.<sup>28</sup> The advantages in this approach clearly lie in the possibility of independent design of sensing and reporting domains and the inability of the reporting units to interact with the nucleic acid matrix, thus reducing erroneous signal generation. Nevertheless, the molecular beacon format in these proof-of-concept experiments was not permitting signal amplification by turnover which prompted us to search for better designs of our orthogonal reporter system. In this study we present a three component system based on hybrid homo-DNA/DNA oligonucleotides, a DNA or RNA analyte and a set of homo-DNA reporter strands that show templated Staudinger reduction of rhodamine-110-azide with multiple turnover and improved signal to noise ratio compared with our previous system.

\*Correspondence to: Christian J. Leumann; Email: leumann@ioc.unibe.ch  
Submitted: 02/11/13; Revised: 03/06/13; Accepted: 03/07/13  
<http://dx.doi.org/10.4161/adna.24227>

## Results

The first series of hybrid oligonucleotides we evaluated for such purposes consisted of a 17-mer homo-DNA core part, which is flanked on both ends by natural DNA ( $\Omega$ -probe, Fig. 2). The homo-DNA core serves as a template to catalyze the reaction of two short homo-DNA reporters (R1 and R2). The two flanking DNA tails are designed to hybridize with the target oligonucleotide. Their length can vary and, as in probe O1 and O2, need not to be symmetric in length. The  $\Omega$ -shaped structure is expected to be formed only in the target bound state, thereby triggering the templated reaction by placing the reactive groups of the homo-DNA reporters in close proximity (Fig. 2). The synthesis of the homo-DNA reporters and hybrid oligonucleotides was performed by standard phosphoramidite chemistry. The sequences used are detailed in Table 1. Homo-DNA reporters were modified with rhodamine-110-azide and triphenylphosphine, respectively, according to a procedure by Ito and coworkers.<sup>17</sup>

With  $\Omega$ -probe O1 and reporter strands R1 and R2 (Table 1) at hand we investigated the fluorescence increase of rhodamine-110 in presence of the matching and single mismatch bearing RNA and DNA targets (Fig. 2; Fig. S1). In order to increase selectivity, the mismatches were designed to appear on the shorter (8-mer) DNA arm of the probe. We observed a match/mismatch discrimination of 4.5 ( $t = 20$  min) for RNA and DNA, which is slightly better compared with our previously reported homo-DNA molecular beacon.<sup>28</sup> Interestingly, the reaction in the presence of a mismatched target is equal to the background reaction in the absence of a target, illustrating the high selectivity of the system (Fig. S2).

We reasoned that the loop structure could impose strain to the homo-DNA pairing domain which might render the templated chemistry less efficient. To prove this hypothesis we incorporated three flexible ethylene glycol-18 spacers into the loop part of the  $\Omega$ -probe (O2). As expected, with O2 mismatch discrimination improved to a ratio of 5.5 ( $t = 20$  min) (Fig. S3).

In search for a higher discriminating and more sensitive detection system we evaluated also another variant, consisting of two independent linear hybrid oligonucleotides (L1, L2) as probe (Fig. 3). Essentially, L1 and L2 correspond to an  $\Omega$ -probe that was split into two halves in the homo-DNA loop region. The DNA-sensing domain was chosen to be of equal length (2 x 10 nt). This design was motivated by the observation that a more flexible loop in the  $\Omega$ -structure improves reaction efficiency. The kinetic analysis of rhodamine-110 fluorescence appearance mediated by L1 and L2 shows reasonable mismatch discrimination for a series of DNA and RNA targets containing single mismatches (match/mismatch ratio around 6.0,  $t = 20$  min, Fig. 3; Fig. S4). The mismatch discrimination could be further improved when the misaligned base-pair was moved toward the center of the DNA sensing arm (Fig. 4, left). Here we find a match/mismatch signal ratio of 19:1 ( $t = 20$  min) and this is similar to assays that are based on templated chemical reactions with DNA or PNA probes, which bind directly to the target.<sup>12,13,26,29</sup>

Having optimized and confirmed the potential of hybrid homo-DNA probes for mismatch detection we turned our

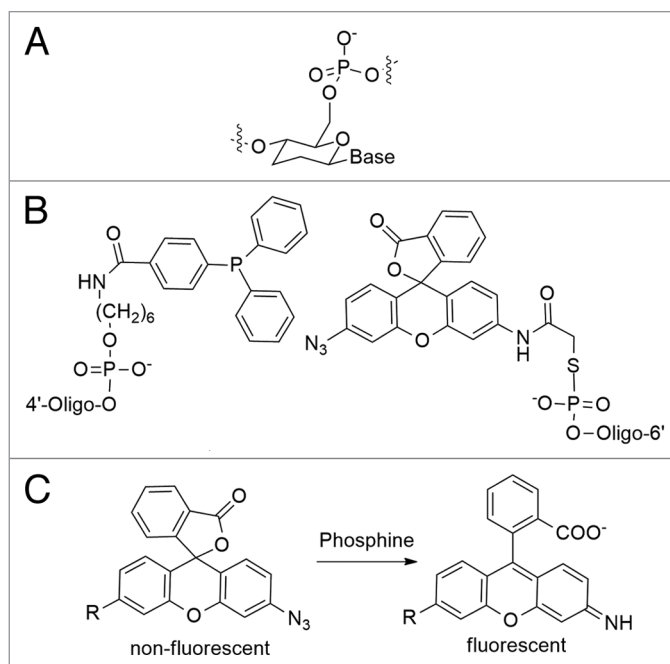


**Figure 1.** (A) Chemical structure of homo-DNA; (B) homo-DNA reporters used in this study, containing either a phosphine unit at the 6'-end or a rhodamine-110-azide unit at the 4'-end; (C) Staudinger reaction of rhodamine-110-azide.

attention toward their ability for fluorescence amplification by multiple turnover of reporter oligonucleotides. Generally, turnover is expected to perform best around the melting temperature ( $T_m$ ) of the reporters, which was determined to be around 33°C for the couple R1 and R2. In order to have reasonably stable duplexes between the hybrid oligonucleotides and the target at these slightly elevated temperatures we used probes with 15-mer DNA sequence tracts for target recognition (L3, L4). Moreover, we also used the tris(2-carboxyethyl)phosphine (TCEP) modified reporter R4 in place of TPP-reporter R1 since it was shown earlier that the lifetime of the aza-ylide intermediate, which is slowing down product release by transiently ligating the probes, is shorter in this case.<sup>14</sup> To evaluate turnover numbers, various sub-stoichiometric amounts of dT11 and corresponding hybrid probes L3 and L4 were investigated at constant reporter concentration (Fig. 4, right).

To quantify the fraction of conversion we used the fully reduced Rhodamine-azide reporter R5 (400 nM) as reference. As expected the highest conversion of more than 80% is obtained using 1 equivalent of target. It is assumed that TCEP reacts partially with oxygen while monitoring fluorescence and therefore rhodamine-110 azide is not fully converted. At a target concentration of 1% (4 nM) we still observe a conversion of 23% after 120 min which is significantly higher than the untemplated background reaction (15% conversion after 120 min). This gives a turnover number of 8 and is thus similar to the value which has been reported by Winsinger and coworkers who used hexameric PNA probes for the same TCEP mediated reduction.<sup>14</sup>

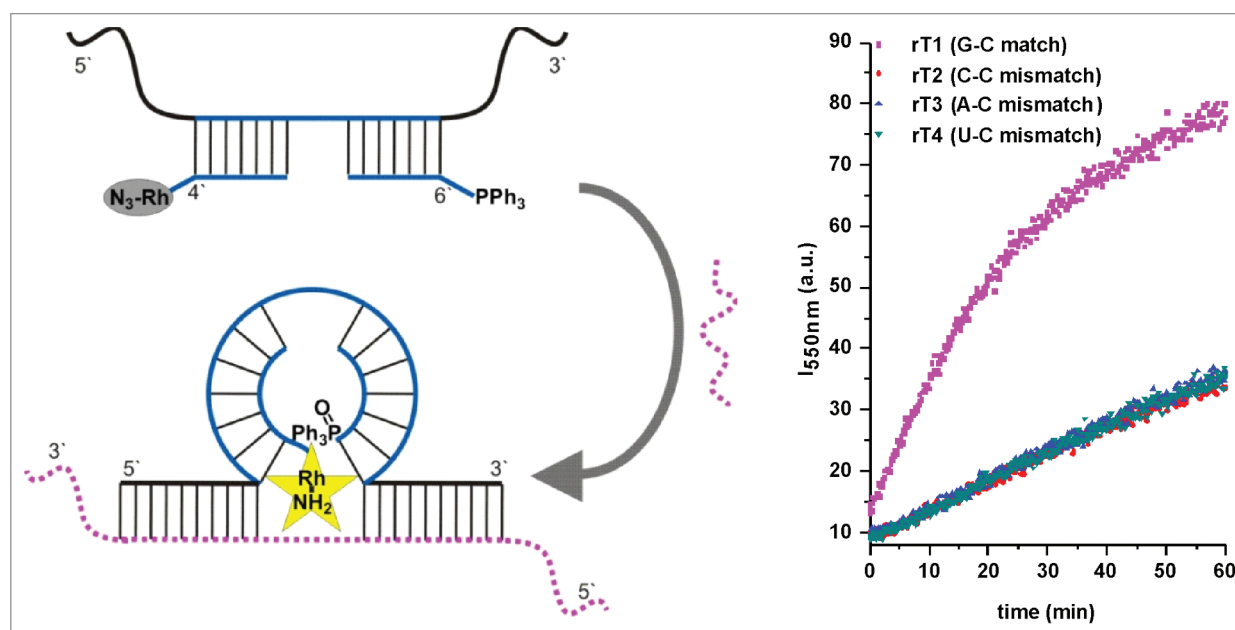


**Figure 2.** Left: Schematic view of the  $\Omega$ -hybrid oligonucleotide for nucleic acid sensing (blue: homo-DNA, black: natural-DNA, dashed magenta: DNA or RNA target). Right: Fluorescence signal development for the templated Staudinger reaction of reporter R1 with R2 on O1 in presence of matched and mismatched RNA targets (rT1–4, **Table 1**). The experiments were performed at 20°C in buffer 1 (50 mM KCl, 10 mM Tris, 3.5 mM MgCl<sub>2</sub>, pH 8.0) with R1 (400 nM), R2 (400 nM), O1 (200 nM) and the indicated targets (200 nM).

## Discussion

Improving the sensitivity and the selectivity of nucleic acid sensing devices is clearly a focus of current interest. Considerable progress in this field has been achieved previously in combining RNA or DNA sensing by complementary oligonucleotides with templated chemical reactions, resulting in fluorescence signal amplification. The assay that we have developed is based on a three to four component system with a chimaeric homo-DNA/DNA probe and two homo-DNA reporter strands. The performance of this system in terms of sensitivity and signal amplification is similar to other systems using the same read out chemistry, based either on natural oligonucleotides or on PNA as probes.<sup>13,14,16,17</sup> Including homo-DNA into the probe, as described here, enables the separation of target recognition and signal generation into orthogonal domains. This bears the advantage of tuning and optimizing parameters relevant for selectivity and sensitivity separately. In other words an efficient homo-DNA reporting sequence can be attached to any DNA sensing domain (symmetric or asymmetric in length) without further sequence design and without the risk of interference with, for example, a cellular nucleic acid matrix. This may specifically prove advantageous when RNA imaging in life cells or animals is envisaged.

## Materials and Methods

**Synthesis of phosphoramidites and building blocks for templated chemistry.** Detailed synthetic procedures are given in the **Supplemental Material** section.

**Oligonucleotide synthesis.** Targets rT1–8 and dT1–11 were purchased from Microsynth (desalted oligonucleotides

used without further purification). All other oligonucleotides (**Table S1**) were prepared from phosphoramidites 1–5 and the natural building blocks for dA, dC, dG, dT (Vivotide). Solid supports (Universal Support 500 was used for homo-DNA Sequences) were purchased from Glen Research. The oligonucleotides were all synthesized on the 1.3  $\mu$ mol scale on a Pharmacia LKB Gene Assembler Special DNA synthesizer. The solutions used for coupling (0.1 M solutions of phosphoramidites in CH<sub>3</sub>CN) as well as for activation, detritylation, capping and oxidation were prepared according to the manufacturer's protocols. As activator 5-(ethylthio)-1H-tetrazole was used (0.25 M in CH<sub>3</sub>CN). The coupling time was extended from 30 sec to 6 min for all phosphoramidites except for the natural dA-, dC-, dG-, dT-building blocks. Otherwise, standard protocols were used. To obtain 3'-thiophosphates the oligonucleotides were synthesized on a 3'-phosphate-CPG solid support (Glen Research), and phenylacetyl disulfide [PADS, 0.2 M solution in pyridine/ACN (1:1)] instead of iodine was used for oxidation. The sulfur oxidation was performed before the capping step with 2 ml of the PADS solution during a period of 90 sec. This protocol is used only for the first phosphoramidite incorporation. After chain elongation and final detritylation, the synthesized oligonucleotides were cleaved from the solid support by ammonia treatment (for details see **Table S1**).

**Oligonucleotide purification.** The oligonucleotides were dissolved in H<sub>2</sub>O (1 ml) and filtered (Titan HPLC-filters, Teflon, 0.45  $\mu$ m, Infochroma AG). Purification was performed by RP-HPLC either on a Source 15 RPC ST (Pharmacia Biotech) or on a Nucleogel RP 300-5 (Macherey-Nagel) column with gradients of buffer B [0.1 M Et<sub>3</sub>N/CH<sub>3</sub>COOH in H<sub>2</sub>O/ACN (1:4), pH 7.0] in buffer A [0.1 M Et<sub>3</sub>N/CH<sub>3</sub>COOH in H<sub>2</sub>O, pH 7.0].

**Table 1.** Sequence composition of probes, reporters and targets

Entry	Sequence <sup>a</sup>	Comment
R1	6'-TPP-gcc tat g-4'	7-mer reporter
R2	6'-ggc acg t-Rhd-N3-4'	7-mer reporter
R3	6'-gca cgt-Rhd-N3-4'	6-mer reporter
R4	6'-TCEP-gcc tat g-4'	7-mer reporter
R5	6'-ggc acg t-Rhd-NH2-4'	7-mer ref
O1	5'-GTC ACT GA acg tgc ctt tca tag gc GAC CAT TTA CGT-3'	Ω-probe
O2	5'-GTC ACT GA acg tgc c (glyc18)3 cat agg c GAC CAT TTA CGT-3'	Ω-probe
L1	5'-CCA AGT TAA G acg tgc c-4'	Linear probe
L2	6'-cat agg c ACC TAT GCA T-3'	Linear probe
L3	5'-TAG GGA ACA AGG GCA acg tgc c-4'	Linear probe
L4	6'-cat agg c AGA GTG TCT GGC TAG-3'	Linear probe
rT1-4	5'-ACG UAA AUG GUC UUU UUC AXU GA-3' (rT1: X = G; rT2: X = C; rT3: X = A; rT4: X = U)	RNA targets
rT5-8	5'-AUG CAU AGG UUU UUC XUA ACU UGG-3' (rT5: X = U; rT6: X = A; rT7: X = C; rT8: X = G)	RNA targets
dT1-4	5'-ACG TAA ATG GTC TTT TTC AXT GA-3' (dT1: X = G; dT2: X = C; dT3: X = A; dT4: X = T)	DNA targets
dT5-8	5'-ATG CAT AGG TTT TTC XTA ACT TGG-3' (dT5: X = T; dT6: X = A; dT7: X = C; dT8: X = G)	DNA targets
dT9	5'-ATG CAT AGG TTT TTC TTA ACT-3'	DNA target
dT10	5'-ATG CAT AGG TTT TTC TTC ACT-3'	DNA target
dT11	5'-CTA GCC AGA CAC TCT TTT TTG CCC TTG TTC CCT A-3'	DNA target

<sup>a</sup>Uppercase letters, natural 2'-deoxyribonucleotides; lowercase letters, homo-DNA nucleotides; TPP, triphenylphosphine; Rhd-N<sub>3</sub>, Rhodamine-110-azide; TCEP, tris(carboxyethyl)phosphine; glyc18, ethylene glycol 18 spacer; underlined characters, mismatched bases.

Detailed conditions for all oligonucleotides are given in **Table S1** in the **Supplemental Material**. After RP-purification the oligonucleotides were desalted over Sep-Pack C18 cartridges (Waters) according to the manufacturer's protocol.

**Post-synthetic derivatization of oligonucleotides.**  
*6'-Triphenylphosphine conjugated oligonucleotide.* (R1): 50 nmol of the corresponding oligonucleotide containing the 6'-NH<sub>2</sub>-C-6 linker were dissolved in 135 μl of 100 mM Na<sub>2</sub>B<sub>4</sub>O<sub>7</sub> buffer (pH 8.5). Then 2 μmol of TPP-ester 7 (see **Supplemental Material**) dissolved in 95 μl DMF were added. The mixture was degassed in an ultrasonic bath (30 sec) to prevent TPP from oxidation and then incubated at 20°C during 1 h in a thermomixer. The mixture was centrifuged (1 min, 14000 rpm) and the supernatant was purified by RP-HPLC.

*4'-Rhodamine azide conjugated oligonucleotides.* (R2, R3) 50 nmol of the respective 4'-phosphothioate modified oligonucleotide were dissolved in 33 μl of 200 mM NaH<sub>2</sub>PO<sub>4</sub> buffer (pH 7.2). Then 2.1 μmol of rhodamine-azide 6 (see **Supplemental Material**) dissolved in 123 μl DMF were added and the reaction mixture was incubated at 20°C over night in a thermomixer. The mixture was centrifuged (1 min, 14000 rpm) and the supernatant was purified by RP-HPLC.

*6'-TCEP-conjugated oligonucleotides.* (R4): 10 μl of dissolved TCEP-diester 8 (see **Supplemental Material**, 0.28 M in DMF) and 10 μl of dissolved NHS (0.36 M in DMF) were added to

10 μl of a solution of EDC (0.36 M in DMF). The mixture was incubated for 1 h at 20°C. Twenty μl thereof were mixed with 75 μl DMF and added to the previously dissolved oligonucleotide [50 nmol in 135 μl of 100 mM Na<sub>2</sub>B<sub>4</sub>O<sub>7</sub> buffer (pH 8.5)]. This mixture was again incubated for 1 h at 20°C and worked up the same way as the TPP modified oligonucleotides.

**Purification of post-synthetically modified oligonucleotides.** All modified oligonucleotides were purified by RP-HPLC after the post-synthetic reaction steps (for detailed conditions see **Table S1**). For TPP and TCEP modified oligonucleotides always two peaks were observed by HPLC. The faster eluting fraction contained the oxidized phosphinoyl whereas the desired phosphine eluted with higher retention time. For an example see the HPLC trace of crude R1 in **Figure S5**. To suppress oxidation of the phosphine containing oligonucleotides during post-HPLC manipulations we used TPP and TCEP modified oligonucleotide fractions after HPLC purification directly in the assays. The oligonucleotides were freshly prepared for each set of experiments, shock frozen and stored in the freezer (-20°C) between single measurements. The rhodamine modified oligonucleotides were desalted with Sep-Pack C18 cartridges (Waters) before further use.

**Oligonucleotide analysis by ESI-MS.** The integrity of the synthesized and purified oligonucleotides was confirmed with ESI-MS (negative ion mode) on a Sciex QSTAR Pulsar mass

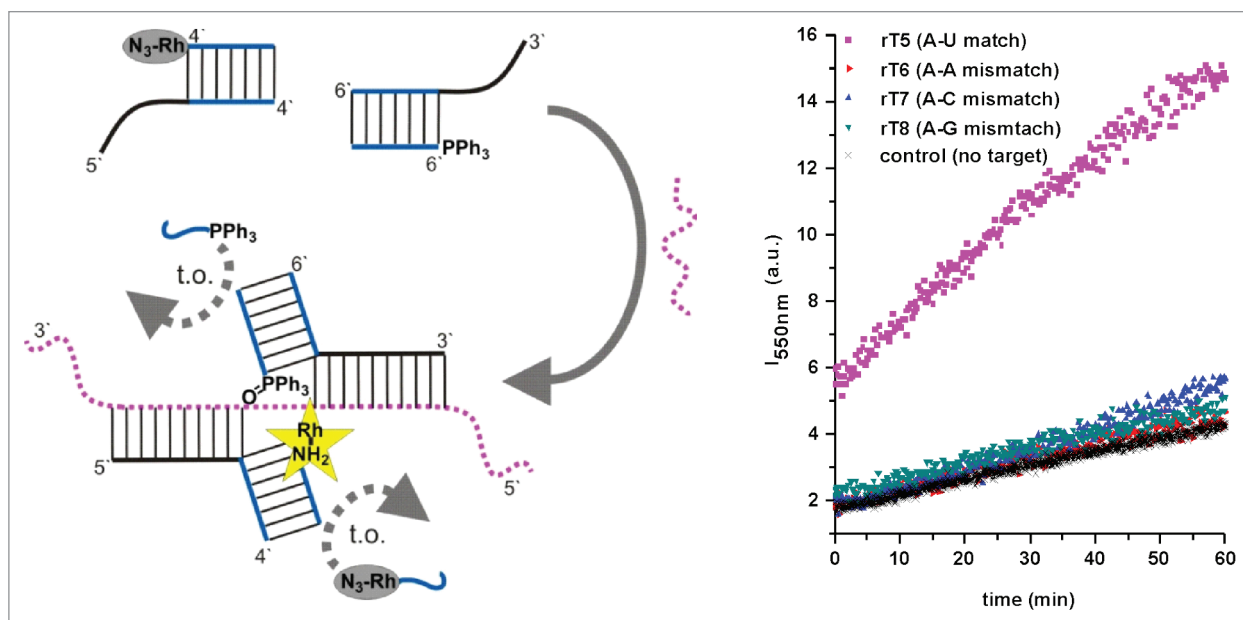


**Figure 3.** Left: Schematic view of linear-hybrid oligonucleotides for nucleic acid sensing with multiple turnover (t.o.) (blue: homo-DNA, black: natural-DNA, dashed magenta: DNA or RNA target). Right: Fluorescence signal development for the templated Staudinger reaction of R1 with R3 on L1 and L2 in presence of matched and mismatched RNA targets (rT5–8). The experiments were performed at 25°C in buffer 2 (50 mM KCl, 10 mM Tris, 3.5 mM MgCl<sub>2</sub>, pH 7.0) with R1 (600 nM), R3 (400 nM), L1, L2 (400 nM) and the indicated targets (400 nM).

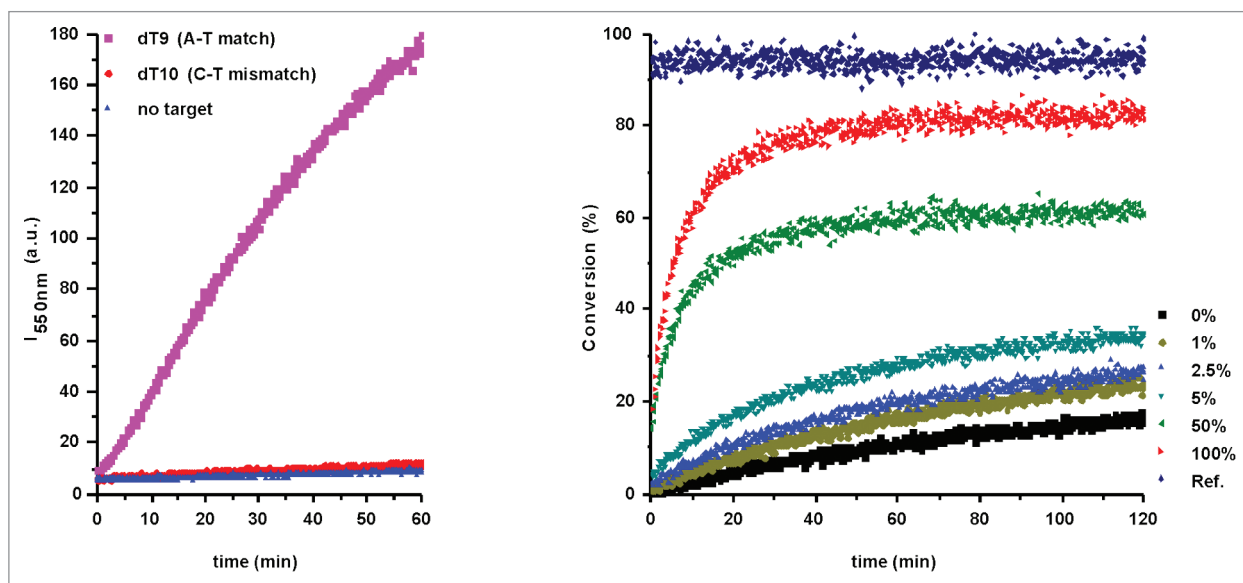


**Figure 4.** Left: Templated reaction on the linear probes L1, L2 for mismatch discrimination (targets dT9, dT10 with mismatch in the center). Experiments were performed at 16°C in buffer 1 (50 mM KCl, 10 mM Tris, 3.5 mM MgCl<sub>2</sub>, pH 8.0) with R1 (400 nM), R2 (400 nM), L1 (200 nM), L2 (200 nM) and the indicated targets (200 nM). Right: Conversion of rhodamine-110-azide in presence of various concentrations of dT11. Experiments were performed at 30°C in buffer 2 (50 mM KCl, 10 mM Tris, 3.5 mM MgCl<sub>2</sub>, pH 7) with R2 (400 nM), R4 (800 nM), L3, L4 and dT11. Concentrations of L3, L4 and dT11 are indicated as percentage of R2. R5 (400 nM) was used as reference.

spectrometer from Applied Biosystems. The corresponding data are summarized in Table S1. TPP-conjugated oligonucleotides contained significant amounts of the oxidized product ( $m/z = M+16$ ).

**Fluorescence measurements.** Fluorescence measurements were performed on a *Cary Eclipse Fluorescence Spectrophotometer*

with a *Cary Temperature Controller* (both from Varian) in fluorescence quartz cuvettes from Hellma with a path length of 10 mm. The photomultiplier voltage was set to 800 V and the emission and excitation slits were set to 5 nm. Measurements were performed with  $\lambda_{\text{ex}} = 490 \text{ nm}$  and  $\lambda_{\text{em}} = 550 \text{ nm}$ .

**Assay setup.** The detailed experimental parameters for all templated reactions are indicated for each experiment in the respective figure captions. The samples were prepared as 1 ml solutions in Eppendorf tubes and mixed before transferring the mixture to the fluorescence cuvettes. TPP and TCEP modified oligonucleotides were always added at last immediately before mixing the sample.

## References

1. Hunziker J, Roth HJ, Bohringer M, Giger A, Diederichsen U, Göbel M, et al. Why Pentose-Nucleic and Not Hexose-Nucleic Acids. 3. Oligo(2',3'-Dideoxy-Beta-D-Glucopyranosyl)Nucleotides - (Homo-DNA) - Base-Pairing Properties. *Helv Chim Acta* 1993; 76:259-352; <http://dx.doi.org/10.1002/hlca.19930760119>.
2. Eschenmoser A. Chemical etiology of nucleic acid structure. *Science* 1999; 284:2118-24; <http://dx.doi.org/10.1126/science.284.5423.2118>; PMID:10381870.
3. Egli M, Pallan PS, Pattanayek R, Wilds CJ, Lubini P, Minasov G, et al. Crystal structure of homo-DNA and nature's choice of pentose over hexose in the genetic system. *J Am Chem Soc* 2006; 128:10847-56; <http://dx.doi.org/10.1021/ja062548x>; PMID:16910680.
4. Bao G, Rhee WJ, Tsurkas A. Fluorescent probes for live-cell RNA detection. *Annu Rev Biomed Eng* 2009; 11:25-47; <http://dx.doi.org/10.1146/annurev-bioeng-061008-124920>; PMID:19400712.
5. Silverman AP, Kool ET. Detecting RNA and DNA with templated chemical reactions. *Chem Rev* 2006; 106:3775-89; <http://dx.doi.org/10.1021/cr050057+>; PMID:16967920.
6. Grossmann TN, Seitz O. DNA-catalyzed transfer of a reporter group. *J Am Chem Soc* 2006; 128:15596-7; <http://dx.doi.org/10.1021/ja0670097>; PMID:17147362.
7. Franzini RM, Kool ET. Efficient nucleic acid detection by templated reductive quencher release. *J Am Chem Soc* 2009; 131:16021-3; <http://dx.doi.org/10.1021/ja904138v>; PMID:19886694.
8. Miller GP, Silverman AP, Kool ET. New, stronger nucleophiles for nucleic acid-templated chemistry: Synthesis and application in fluorescence detection of cellular RNA. *Bioorg Med Chem* 2008; 16:56-64; <http://dx.doi.org/10.1016/j.bmc.2007.04.051>; PMID:17502150.
9. Grossmann TN, Seitz O. Nucleic acid templated reactions: consequences of probe reactivity and readout strategy for amplified signaling and sequence selectivity. *Chemistry* 2009; 15:6723-30; <http://dx.doi.org/10.1002/chem.200900025>; PMID:19496097.
10. Cai J, Li X, Yue X, Taylor JS. Nucleic acid-triggered fluorescent probe activation by the Staudinger reaction. *J Am Chem Soc* 2004; 126:16324-5; <http://dx.doi.org/10.1021/ja0452626>; PMID:15600325.
11. Franzini RM, Kool ET. Organometallic activation of a fluorogen for templated nucleic acid detection. *Org Lett* 2008; 10:2935-8; <http://dx.doi.org/10.1021/ol800878b>; PMID:18549220.

## Disclosure of Potential Conflicts of Interest

No potential conflicts of interest were disclosed.

## Supplemental Material

Supplemental materials may be found here:

<http://www.landesbioscience.com/journals/artificialdna/article/24227/>

12. Franzini RM, Kool ET. 7-Azidomethoxy-coumarins as profluorophores for templated nucleic acid detection. *Chembiochem* 2008; 9:2981-8; <http://dx.doi.org/10.1002/cbic.200800507>; PMID:19035374.
13. Pianowski ZL, Winssinger N. Fluorescence-based detection of single nucleotide permutation in DNA via catalytically templated reaction. *Chem Commun (Camb)* 2007; 3820-2:3820-2; <http://dx.doi.org/10.1039/b709611a>; PMID:18217658.
14. Pianowski Z, Gorska K, Oswald L, Merten CA, Winssinger N. Imaging of mRNA in live cells using nucleic acid-templated reduction of azidorhodamine probes. *J Am Chem Soc* 2009; 131:6492-7; <http://dx.doi.org/10.1021/ja809656k>; PMID:19378999.
15. Shibata A, Abe H, Ito M, Kondo Y, Shimizu S, Aikawa K, et al. DNA templated nucleophilic aromatic substitution reactions for fluorogenic sensing of oligonucleotides. *Chem Commun (Camb)* 2009; 6586-8:6586-8; <http://dx.doi.org/10.1039/b912896d>; PMID:19865658.
16. Furukawa K, Abe H, Wang J, Uda M, Koshino H, Tsuneda S, et al. Reduction-triggered red fluorescent probes for dual-color detection of oligonucleotide sequences. *Org Biomol Chem* 2009; 7:671-7; <http://dx.doi.org/10.1039/b817228e>; PMID:19194582.
17. Abe H, Wang J, Furukawa K, Oki K, Uda M, Tsuneda S, et al. A reduction-triggered fluorescence probe for sensing nucleic acids. *Bioconjug Chem* 2008; 19:1219-26; <http://dx.doi.org/10.1021/bc800014d>; PMID:18476727.
18. Röthlingshöfer M, Gorska K, Winssinger N. Nucleic acid templated uncaging of fluorophores using Ru-catalyzed photoreduction with visible light. *Org Lett* 2012; 14:482-5; <http://dx.doi.org/10.1021/ol203029t>; PMID:22206275.
19. Röthlingshöfer M, Gorska K, Winssinger N. Nucleic acid-templated energy transfer leading to a photorelease reaction and its application to a system displaying a nonlinear response. *J Am Chem Soc* 2011; 133:18110-3; <http://dx.doi.org/10.1021/ja2086504>; PMID:22004511.
20. Prusty DK, Kwak M, Wildeman J, Herrmann A. Modular assembly of a Pd catalyst within a DNA scaffold for the amplified colorimetric and fluorimetric detection of nucleic acids. *Angew Chem Int Ed Engl* 2012; 51:11894-8; <http://dx.doi.org/10.1002/anie.201206006>; PMID:23076826.
21. Gorska K, Manicardi A, Barluenga S, Winssinger N. DNA-templated release of functional molecules with an azide-reduction-triggered immolative linker. *Chem Commun (Camb)* 2011; 47:4364-6; <http://dx.doi.org/10.1039/c1cc10222b>; PMID:21369617.
22. Gorska K, Keklikoglou I, Tschulena U, Winssinger N. Rapid fluorescence imaging of miRNAs in human cells using templated Staudinger reaction. *Chem Sci* 2011; 2:1969-75; <http://dx.doi.org/10.1039/c1sc00216c>.
23. Meguellati K, Koripelly G, Ladame S. DNA-templated synthesis of trimethine cyanine dyes: a versatile fluorogenic reaction for sensing G-quadruplex formation. *Angew Chem Int Ed Engl* 2010; 49:2738-42; <http://dx.doi.org/10.1002/anie.201000291>; PMID:20229556.
24. Chen XH, Roloff A, Seitz O. Consecutive signal amplification for DNA detection based on de novo fluorophore synthesis and host-guest chemistry. *Angew Chem Int Ed Engl* 2012; 51:4479-83; <http://dx.doi.org/10.1002/anie.201108845>; PMID:22441837.
25. Grossmann TN, Strohbach A, Seitz O. Achieving turnover in DNA-templated reactions. *Chembiochem* 2008; 9:2185-92; <http://dx.doi.org/10.1002/cbic.200800290>; PMID:18752239.
26. Furukawa K, Abe H, Hibino K, Sako Y, Tsuneda S, Ito Y. Reduction-triggered fluorescent amplification probe for the detection of endogenous RNAs in living human cells. *Bioconjug Chem* 2009; 20:1026-36; <http://dx.doi.org/10.1021/bc900040t>; PMID:19374406.
27. Crey-Desbiolles C, Ahn DR, Leumann CJ. Molecular beacons with a homo-DNA stem: improving target selectivity. *Nucleic Acids Res* 2005; 33:e77; <http://dx.doi.org/10.1093/nar/gni076>; PMID:15879349.
28. Stoop M, Leumann CJ. Homo-DNA templated chemistry and its application to nucleic acid sensing. *Chem Commun (Camb)* 2011; 47:7494-6; <http://dx.doi.org/10.1039/c1cc11469g>; PMID:21552601.
29. Abe H, Kool ET. Destabilizing universal linkers for signal amplification in self-ligating probes for RNA. *J Am Chem Soc* 2004; 126:13980-6; <http://dx.doi.org/10.1021/ja046791c>; PMID:15506759.